Quantum Monte Carlo Calculations in Solids with Downfolded Hamiltonians

Fengjie Ma, Wirawan Purwanto, Shiwei Zhang, and Henry Krakauer
Department of Physics, College of William and Mary, Williamsburg, Virginia 23187, USA

(Received 30 November 2014; published 1 June 2015)

We present a combination of a downfolding many-body approach with auxiliary-field quantum Monte Carlo (AFQMC) calculations for extended systems. Many-body calculations operate on a simpler Hamiltonian which retains material-specific properties. The Hamiltonian is systematically improvable and allows one to dial, in principle, between the simplest model and the original Hamiltonian. As a by-product, pseudopotential errors are essentially eliminated using frozen orbitals constructed adaptively from the solid environment. The computational cost of the many-body calculation is dramatically reduced without sacrificing accuracy. Excellent accuracy is achieved for a range of solids, including semiconductors, ionic insulators, and metals. We apply the method to calculate the equation of state of cubic BN under ultrahigh pressure, and determine the spin gap in NiO, a challenging prototypical material with strong electron correlation effects.

DOI: 10.1103/PhysRevLett.114.226401 PACS numbers: 71.10.-w, 02.70.Ss, 71.15.Nc

Developing accurate and efficient computational approaches for quantum matter has been a long-standing challenge. Parameter-free, material-specific many-body calculations are needed where simpler methods, such as those based on density functional theory (DFT) [1] or perturbative approaches, break down. Examples range from strongly correlated materials, such as transition metal oxides, to bond stretching or bond breaking in otherwise moderately correlated systems. Significant progress has been made with wave function based methods such as density matrix renormalization group (DMRG) [2], coupled cluster [CCSD(T)], and full configuration interaction quantum Monte Carlo (FCIQMC) [3]. However, their computational cost tends to scale steeply with system size. Quantum Monte Carlo (QMC) calculation has become increasingly important in this regard [4–12], although systematic and routine applications of QMC calculations in realistic materials still face major challenges. Here we present an approach which overcomes several of the obstacles with QMC calculations, and advances the capabilities of nonperturbative ground-state calculations in correlated materials in general.

Our approach leverages the accuracy, versatility, and favorable scaling of the auxiliary-field quantum Monte Carlo (AFQMC) method [5,13,14], and combines it with downfolding, which is often employed to construct reduced Hamiltonians from band structure calculations for model studies [15,16]. A compact and systematic basis set is obtained for the target periodic solids, including magnetic systems, by truncating DFT orbitals. This allows QMC calculations to be performed with a much simpler Hamiltonian while retaining material-specific properties. The simplification, often with drastic reduction in computational cost, can extend the reach of *ab initio* computations to more complex materials. A large gain in statistical accuracy often results as well, because of the smaller range of energy scales (or many fewer degrees of freedom) which need to be sampled stochastically in the downfolded Hamiltonian.

Two other key advantages follow as a result of this approach. First, by varying the cutoff that controls the truncation of the basis orbitals, one could in principle dial between the original full-basis Hamiltonian and the simplest model. QMC calculations can be performed at each stage. This allows a systematically improvable set of calculations that connect simple models to full materials specificity. Second, the approach introduces a new way for treating core electrons, which has been a critical issue in QMC calculations. Significant errors are often present with the use of pseudopotentials (PSPs) in QMC calculations [17,18], due to (i) inherent limitations in the accuracy of such PSPs (single-projector, generated in an atomic environment, from independent-electron calculations) [19–21], and (ii) approximations in how the PSP has to be implemented in standard diffusion Monte Carlo (DMC) calculations [4,22]. A recent DMC study of high-pressure BN showed [23] that all-electron calculations were required, which in most materials would not be practical. In our approach a frozen-core (FC) treatment [24] eliminates the difficulty.

The most fundamental issue in computations of electron correlation effects is accuracy. For QMC calculations, the fermion sign problem must, in all but a few special cases, be controlled with an approximation. The AFQMC framework, by carrying out the random walks in nonorthogonal Slater determinant space, has shown to lead to an approximation which is more accurate and less dependent on the trial wave function [5,7,12,21,25,26]. The method proposed here provides an approach to seamlessly integrate these advances in the study of solids. We illustrate the approach by obtaining accurate equilibrium properties in a range of solids, including semiconductors, ionic insulators, and metals. We then apply it to tackle two challenging problems, the high pressure equation of state (EOS) of cubic BN (pressure calibration) and accurate determination of the spin gap in strongly correlated NiO.

The construction of the downfolded Hamiltonian begins with a standard DFT calculation for the target system. This is done using a plane wave basis with PSPs. (Arbitrarily hard PSPs can be employed to eliminate transferability errors of conventional norm-conserving PSPs [24], at little additional computational cost in the ensuing many-body calculations.) Plane waves are desirable at this stage, because they provide an unbiased representation of the many-body Hamiltonian. We then use the Kohn-Sham (KS) orbitals as the basis set, tuned to eliminate less physically relevant high-energy virtual states and low-energy core states, as illustrated in Fig. 1(a). Expressed in this basis, the effective downfolded Hamiltonian is given by

$$\hat{H} = \sum_{i,j} K_{ij} c_i^\dagger c_j + \frac{1}{2} \sum_{i,j,k,l} V_{ijkl} c_i^\dagger c_j^\dagger c_k c_l. \tag{1}$$

The matrix elements of one-body (and constant) term $\hat{K}$ and two-body interaction term $\hat{V}$ are

$$K_{ij} = \langle \chi_i | \hat{K} | \chi_j \rangle; \qquad V_{ijkl} = \langle \chi_i \chi_j | \hat{V} | \chi_k \chi_l \rangle, \tag{2}$$

where $|\chi_i\rangle$ is a KS orbital, and the labels i, j, k, and l all run in the truncated basis set. The matrix elements, which encode the periodicity and the Coulomb interaction in the underlying supercell [21], can be conveniently computed using fast Fourier transforms, as the orbitals χ are given in plane waves. The computational cost of evaluating these matrix elements is negligible compared to the subsequent many-body simulations. We use twist boundary conditions [27] on the supercell. For inversion-symmetric systems, all the matrix elements are *real* under any twist $\mathbf{k}$. The core states can be frozen in the corresponding KS orbitals of the solid; two-body core-valence interactions appear as one-body ion-valence terms in K_{ij} and core-only interactions (one-body and two-body) contribute a constant [24].

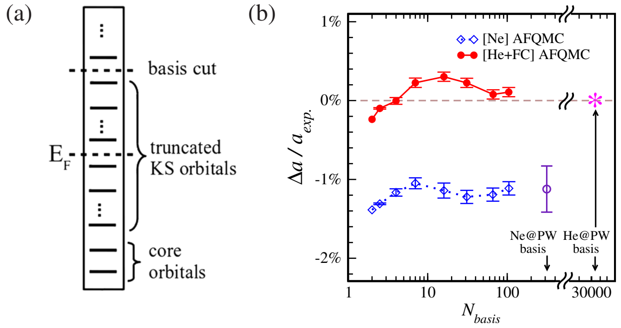

FIG. 1 (color online). (a) Illustration for basis downfolding. Solid black lines represent DFT KS orbitals. A compact basis is constructed with DFT-KS orbitals, by neglecting the less physically relevant high-energy states above a truncation energy. Deep core electrons can be frozen at the mean-field level by a frozen-core treatment. (b) Error in the calculated lattice constant in Si vs basis size. Results with standard Ne-core and a highly accurate He-core PSP plus FC are both shown. For the Ne-core PSP, the full plane wave AFQMC result is indicated by the indigo open circle. For the He-core PSP, the number of plane waves required in the full calculation is indicated (note logarithmic scale).

The downfolded Hamiltonian defined in Eq. (1) is then treated using the phaseless AFQMC method [13] but in the molecular formalism [14,28], which can handle any one-particle basis functions. The approach is illustrated for fcc Si in Fig. 1(b), which shows the convergence of the calculated equilibrium lattice constant. Results are shown for both Ne- and He-core PSPs [29]. With the Ne-core PSP, each Si atom contributes four electrons, and there are no "core electrons" in the diagram in Fig. 1(a). The basis cut controls the number of KS orbitals in the truncated basis, N_{basis}. When all states are retained in the truncation, the KS orbital basis is just a unitary transformation of the original plane wave basis. As N_{basis} is increased, the result converges to the full plane wave AFQMC result. The statistical error bar with the downfolded Hamiltonian is much smaller, however, because many fewer auxiliary fields need to be sampled [21,28]. With the He-core PSP, very small radial cutoffs (0.54, 0.68, and 0.54 bohr for s, p, and d channels, respectively) were used, which resulted in a large plane wave cutoff $E_{\text{cut}} = 600$ Ry. The $2s$ and $2p$ electrons are then treated as "core electrons," frozen in their KS orbitals. As seen in Fig. 1(b), this approach (He-core plus FC) eliminates the 1.2% error in the calculated lattice constant from the Ne-core PSP. Furthermore, the calculation reaches convergence with ~100 basis functions, more than 2 orders of magnitude smaller than would be required in the full plane wave calculation. We further illustrate the downfolding procedure and its convergence in the Supplemental Material with a detailed calculation of the EOS for diamond [30].

The basis choice and truncation method are not unique. Possible truncation choices include a fixed number of basis functions, a fixed cutoff energy, a fixed ratio to the full basis, etc. We find that the first choice leads to the most rapid convergence in our EOS calculations. There is also considerable freedom in the choice of underlying basis. In spin-polarized systems, we generate a spin-consistent basis set by diagonalizing the $2N_{\text{basis}} \times 2N_{\text{basis}}$ overlap matrix formed by $\langle \chi_i^\sigma | \chi_j^{\sigma'} \rangle$, where σ and σ' are spin indices. The resulting eigenfunctions corresponding to the largest N_{basis} eigenvalues are used as new "KS orbitals," which leads to an unbiased basis set and much faster convergence, as illustrated for NiO below. Similarly, localization strategies could be applied to generate more efficient basis sets [34–36].

We first apply the AFQMC downfolding approach to two semiconductors Si and C, two metals Na and Al, an ionic crystal NaCl, and BN, whose high-pressure EOS is further studied below for pressure calibration. Figure 2 summarizes the calculated equilibrium properties and

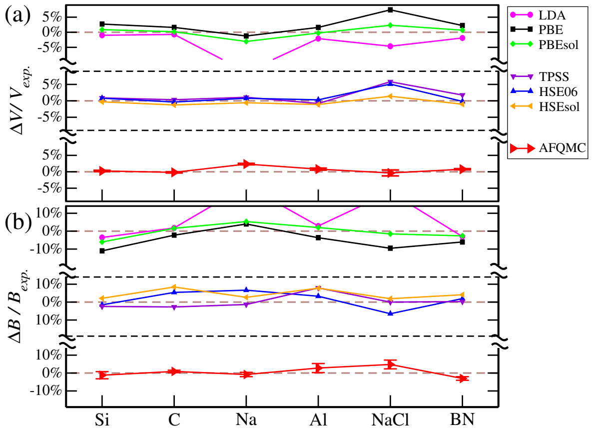

FIG. 2 (color online). Summary of calculated equilibrium volumes (a) and bulk moduli (b), shown as relative errors from experiment. Selected DFT results are also shown for reference. Zero-point effects have been subtracted from the experiments [38,39].

compares them with experiment [37]. The calculations for NaCl and BN were analogous to those for Si and C. The calculations in bcc Na and fcc Al used twist averaging over 90 random **k** points [27]. He-core PSPs were used for Na and Al, together with the FC treatment as described for Si. This makes a major difference in both NaCl and Na. With a Ne-core PSP, the equilibrium volume is underestimated by ~30% in Na, for example. The error is eliminated by the FC approach, which allows the semicore $2s$ and $2p$ electrons to fully relax in the *target environment of the solid* at the DFT level, before freezing them in the corresponding KS orbitals in the many-body calculation.

The agreement between the downfolding AFQMC calculations and experiments [38,40–42] is excellent. For reference, some representative DFT results are shown in Fig. 2: the top panels in (a) and (b) include results from the widely used local-density (LDA) and generalized gradient (GGA, with two flavors, PBE and a variant which is specially designed for solids and surfaces, PBEsol) approximations [43–45]; the middle panels sample more recent developments in DFT, with a meta-GGA (TPSS) and two flavors of hybrid functionals (HSE06 and HSEsol) [38,40–42], which are highly accurate in many conventional systems but often involve empirical parameters. The AFQMC results (bottom panels) demonstrate that the new approach provides an *ab initio*, parameter-free, many-body framework that is consistently accurate. The calculations used single-determinant trial wave functions taken directly from LDA or GGA to control the sign or phase problem of the random walks in Slater determinant space [5,13]. The systematic error from this approximation, based on extensive prior benchmarks [12,13,21,25], is expected to be essentially negligible in these systems, in accord with the results in the figure. The largest uncertainty arises in NaCl and is statistical in nature. Different from the other systems, the ionic character results in valence states localized on the Cl atom. The high-energy virtual KS orbitals, which are used to capture the effect of electron interactions, are free-electron-like, however. As a result, convergence of the EOS is slow and an extrapolation with respect to $1/N_{\text{basis}}$ was needed to reach the complete basis set limit, resulting in larger uncertainty. Clearly, this can be improved by using Wannier or other localized orbitals in the downfolding.

In a more demanding test, we apply the downfolding AFQMC method to obtain the EOS of cubic BN for pressures up to 900 GPa ($V \sim 0.5V_{eq}$). This system has been identified as a promising material for an ultrahigh pressure calibration scale [23,46]. A recent DMC study stressed the need for all-electron (AE) calculations in order to obtain reliable results at high pressures [23]. The difficulty underscores the PSP transferability problem discussed above in the context of Na and Si, and is exacerbated by the need to apply a locality approximation in DMC calculations to treat nonlocal PSPs [4,22]. The AE treatment would be difficult to realize for heavier atoms. Our calculations freeze the $1s$ electrons in their KS orbitals in the supercell at each volume, using extremely hard "zero-electron-core" PSPs for B and N in the downfolding procedure [47]. In most cases ~55 states/atom were used, but larger N_{basis} calculations were done at selected volumes to extrapolate the EOS to the complete basis set limit. We applied finite-temperature corrections following Ref. [23]. The calculations were done with $\mathbf{k} = (0.5, 0.5, 0.0)$ for 8- and 16-atom supercells, with one- and two-body finite-size corrections as discussed earlier; we have confirmed that residual errors are negligible compared to the final estimated error band, especially in the high-pressure regime. As seen in Fig. 3, the calculated EOS at low pressures is in excellent agreement with experiments [39,48–50]. The calculated equilibrium lattice constant, 6.820(3) bohr, is consistent with experimental measurements of 6.802 bohr (zero-point energy removed), as shown in the inset. The EOS at low pressures shows small but discernible discrepancies with DMC results. Possible origins include differences in the finite-temperature corrections [51], or DMC fixed-node errors, and will require further investigation. At high pressures, the two QMC results are in good agreement, providing a consistent *ab initio* pressure calibration.

As a final application, we determine the spin gap between the ferromagnetic (FM) state and the antiferromagnetic (AFM-II) ground state in NiO. Understanding and predicting magnetic properties of transition-metal oxides epitomizes the challenge of computations in quantum matter. NiO is a prototypical system for strong electron correlations. Many-body calculations of the spin gap have been limited, and DFT-based methods have yielded widely varying values [52]. We use Ne-core and He-core PSPs for Ni and O, respectively. The downfolded Hamiltonian treats the Ni $3s, 3p, 3d, 4s$, and O $2s, 2p$ electrons. A rhombohedral supercell with a lattice constant of 4.17 Å containing two formula units is used. To reduce one-body finite-size

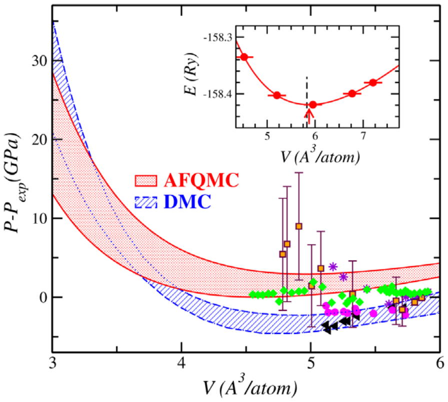

FIG. 3 (color online). Pressure calibration and EOS in cubic BN. The main graph displays the calculated pressure vs volume at room temperature, using the fitted experimental curve of Ref. [39] (green diamond symbols) as a pressure reference. Symbols represent different experiments, including green diamonds [39], orange squares [48], magenta circles, black triangles [49], and violet stars [50]. The shading gives the overall statistical uncertainties in the calculations. The all-electron DMC results are from Ref. [23]. The inset shows the $T = 0$ K EOS near equilibrium from the AFQMC calculations. The calculated equilibrium position is shown by the arrow. The vertical line indicates the experimental value [39,49].

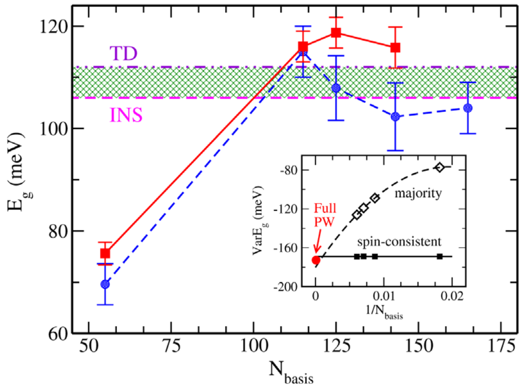

FIG. 4 (color online). Spin gap in NiO, and comparison with experiment. A smaller set of calculations (blue circles), averaging over two **k** points, confirms convergence with respect to basis set cutoff N_{basis}. Calculations averaging over a $4 \times 4 \times 4$ Monkhorst-Pack grid (red squares) are used to obtain the final results. The shaded bar represents the experimental range: inelastic neutron scattering (INS) [54] (bottom line) and thermodynamic (TD) measurements [55] (top line). The inset illustrates the much faster convergence enabled by the spin-consistent basis set (see text) than using the KS orbitals from the majority spin.

effects, we used twist averaging with a $4 \times 4 \times 4$ Monkhorst-Pack grid [53]. (A recent study [3] by FCIQMC and coupled-cluster methods, with calculations at $\mathbf{k} = \Gamma$, obtained a gap value ~0.96 eV.) One- and two-body finite-size corrections [33] are then applied to the many-body results. (Two-body finite-size effects are greatly reduced by cancellation, because the two phases share the same supercell.) The total CPU time required to obtain the $4 \times 4 \times 4$ result in the largest basis set is ~0.48 million Cray XK6 (Titan) core hours. In the downfolding we use the spin-consistent basis sets discussed earlier. In the inset in Fig. 4, the variational gap value from the single-determinant trial wave functions is shown vs the number of basis functions, for both the spin-consistent basis set and one which uses truncated KS orbitals of the majority spin. Both converge to the same infinite basis-set limit, as expected, but the former greatly accelerates convergence. Note that the variational gap (which has been averaged over **k** points) is actually negative; i.e., the trial wave functions identify the incorrect phase for the ground state. The AFQMC calculations correctly recover from these, and yield a final estimate of the gap of 116(3) meV, in good agreement with experiments [54,55].

In summary, we have presented an approach for extended systems combining systematic downfolding Hamiltonians with the AFQMC method. As a first test, parameter-free calculations of equilibrium properties are demonstrated in semiconductors, metals, and ionic insulators. QMC PSP errors are eliminated without (prohibitive) all-electron calculations, as demonstrated in BN. The spin gap in strongly correlated NiO is accurately determined. The approach drastically reduces complexity and computational cost, and greatly extends the reach of *ab initio*, nonperturbative, many-body computations in complex materials. Furthermore, the framework provides a tunable connection between the full materials-specific Hamiltonian and simplified models. The downfolding approach can be generalized to carry out excited state and many-body band structure calculations, which was recently formulated [12] in the plane wave AFQMC method. A large number of applications are possible within the present form. Further improvements, for example by using localized virtual states or optimizing the orbitals with respect to the environments, will lead to even more general and powerful approaches.

This work is supported by DOE (Grands No. DE-SC0008627 and No. DE-SC0001303), NSF (Grand No. DMR-1409510), and ONR (Grand No. N000141211042). An award of computer time was provided by the Innovative and Novel Computational Impact on Theory and Experiment (INCITE) program, using resources of the Oak Ridge Leadership Computing Facility at the Oak Ridge National Laboratory, which is supported by the Office of Science of the U.S. Department of Energy under Contract No. DE-AC05-00OR22725. We also acknowledge computing support from the computational facilities at the College of William and Mary.

---

[1] W. Kohn, Rev. Mod. Phys. **71**, 1253 (1999).
[2] S. R. White, Phys. Rev. Lett. **69**, 2863 (1992); Y. Kurashige, G. K.-L. Chan, and T. Yanai, Nat. Chem. **5**, 660 (2013);

S. Sharma, K. Sivalingam, F. Neese, and G. K.-L. Chan, Nat. Chem. **6**, 927 (2014); J. Yang, W. Hu, D. Usvyat, D. Matthews, M. Schütz, and G. K.-L. Chan, Science **345**, 640 (2014); S. Wouters and D. V. Neck, Eur. Phys. J. D **68**, 272 (2014).

[3] G. H. Booth, A. Grüneis, G. Kresse, and A. Alavi, Nature (London) **493**, 365 (2013).

[4] W. M. C. Foulkes, L. Mitas, R. J. Needs, and G. Rajagopal, Rev. Mod. Phys. **73**, 33 (2001).

[5] S. Zhang, in *Auxiliary-Field Quantum Monte Carlo for Correlated Electron Systems*, edited by E. Pavarini, E. Koch, and U. Schollwöck, Emergent Phenomena in Correlated Matter: Modeling and Simulation, Vol. 3 (Verlag des Forschungszentrum, Jülich, 2013).

[6] W. A. Al-Saidi, S. Zhang, and H. Krakauer, J. Chem. Phys. **127**, 144101 (2007).

[7] W. Purwanto, S. Zhang, and H. Krakauer, J. Chem. Phys. **142**, 064302 (2015).

[8] L. Shulenburger and T. R. Mattsson, Phys. Rev. B **88**, 245117 (2013).

[9] J. Kolorenč and L. Mitas, Rep. Prog. Phys. **74**, 026502 (2011).

[10] L. K. Wagner, J. Phys. Condens. Matter **19**, 343201 (2007).

[11] L. K. Wagner and P. Abbamonte, Phys. Rev. B **90**, 125129 (2014).

[12] F. Ma, S. Zhang, and H. Krakauer, New J. Phys. **15**, 093017 (2013).

[13] S. Zhang and H. Krakauer, Phys. Rev. Lett. **90**, 136401 (2003).

[14] W. A. Al-Saidi, S. Zhang, and H. Krakauer, J. Chem. Phys. **124**, 224101 (2006).

[15] P. Löwdin, J. Chem. Phys. **19**, 1396 (1951).

[16] O. K. Andersen, A. I. Liechtenstein, O. Jepsen, and F. Paulsen, J. Phys. Chem. Solids **56**, 1573 (1995).

[17] S. Sorella, M. Casula, L. Spanu, and A. Dal Corso, Phys. Rev. B **83**, 075119 (2011).

[18] R. G. Hennig, A. Wadehra, K. P. Driver, W. D. Parker, C. J. Umrigar, and J. W. Wilkins, Phys. Rev. B **82**, 014101 (2010).

[19] J. R. Trail and R. J. Needs, J. Chem. Phys. **122**, 174109 (2005).

[20] M. Burkatzki, C. Filippi, and M. Dolg, J. Chem. Phys. **126**, 234105 (2007).

[21] M. Suewattana, W. Purwanto, S. Zhang, H. Krakauer, and E. J. Walter, Phys. Rev. B **75**, 245123 (2007).

[22] L. Mitáš, E. L. Shirley, and D. M. Ceperley, J. Chem. Phys. **95**, 3467 (1991).

[23] K. P. Esler, R. E. Cohen, B. Militzer, J. Kim, R. J. Needs, and M. D. Towler, Phys. Rev. Lett. **104**, 185702 (2010).

[24] W. Purwanto, S. Zhang, and H. Krakauer, J. Chem. Theory Comput. **9**, 4825 (2013).

[25] W. Purwanto, H. Krakauer, and S. Zhang, Phys. Rev. B **80**, 214116 (2009).

[26] C.-C. Chang and S. Zhang, Phys. Rev. Lett. **104**, 116402 (2010).

[27] C. Lin, F. H. Zong, and D. M. Ceperley, Phys. Rev. E **64**, 016702 (2001).

[28] W. Purwanto, H. Krakauer, Y. Virgus, and S. Zhang, J. Chem. Phys. **135**, 164105 (2011).

[29] E. J. Walter, Opium: Pseudopotential Generation Project, http://opium.sourceforge.net.

[30] See Supplemental Material at http://link.aps.org/supplemental/10.1103/PhysRevLett.114.226401 for an illustration of downfolding and convergence in fcc diamond, which includes Refs. [31–33].

[31] F. D. Murnaghan, Proc. Natl. Acad. Sci. U.S.A. **30**, 244 (1944).

[32] H. Kwee, S. Zhang, and H. Krakauer, Phys. Rev. Lett. **100**, 126404 (2008).

[33] F. Ma, S. Zhang, and H. Krakauer, Phys. Rev. B **84**, 155130 (2011).

[34] I.-M. Høyvik, K. Kristensen, T. Kjærgaard, and P. Jørgensen, Theor. Chem. Acc. **133**, 1417 (2014).

[35] A. Grüneis, G. H. Booth, M. Marsman, J. Spencer, A. Alavi, and G. Kresse, J. Chem. Theory Comput. **7**, 2780 (2011).

[36] N. Marzari, A. A. Mostofi, J. R. Yates, I. Souza, and D. Vanderbilt, Rev. Mod. Phys. **84**, 1419 (2012).

[37] The total number of truncated basis functions varied from ~150 to ~470 in these calculations.

[38] L. Schimka, J. Harl, and G. Kresse, J. Chem. Phys. **134**, 024116 (2011).

[39] F. Datchi, A. Dewaele, Y. Le Godec, and P. Loubeyre, Phys. Rev. B **75**, 214104 (2007).

[40] V. N. Staroverov, G. E. Scuseria, J. Tao, and J. P. Perdew, Phys. Rev. B **69**, 075102 (2004).

[41] V. N. Staroverov, G. E. Scuseria, J. Tao, and J. P. Perdew, Phys. Rev. B **78**, 239907(E) (2008).

[42] P. Hao, Y. Fang, J. Sun, G. I. Csonka, P. H. T. Philipsen, and J. P. Perdew, Phys. Rev. B **85**, 014111 (2012).

[43] J. P. Perdew and A. Zunger, Phys. Rev. B **23**, 5048 (1981).

[44] J. P. Perdew, K. Burke, and M. Ernzerhof, Phys. Rev. Lett. **77**, 3865 (1996).

[45] J. P. Perdew, A. Ruzsinszky, G. I. Csonka, O. A. Vydrov, G. E. Scuseria, L. A. Constantin, X. Zhou, and K. Burke, Phys. Rev. Lett. **100**, 136406 (2008).

[46] Y. Tian *et al.*, Nature (London) **493**, 385 (2013).

[47] The radial cutoffs are 0.58 bohr for s and p channels of B, and 0.61 bohr for those of N, resulting in plane wave cutoff 600 Ry.

[48] E. Knittle, R. M. Wentzcovitch, R. Jeanloz, and M. L. Cohen, Nature (London) **337**, 349 (1989).

[49] A. F. Goncharov, J. C. Crowhurst, J. K. Dewhurst, S. Sharma, C. Sanloup, E. Gregoryanz, N. Guignot, and M. Mezouar, Phys. Rev. B **75**, 224114 (2007).

[50] V. L. Solozhenko, D. Häusermann, M. Mezouar, and M. Kunz, Appl. Phys. Lett. **72**, 1691 (1998).

[51] Finite temperature contribution is obtained from the difference between our standard 0K DFT calculation and the room temperature DFT result in Ref. [23]. Both of the PSPs are generated with OPIUM using the same type of exchange-correlation functional (WCGGA). The radial cutoffs are 1.08 bohr for s, p, and d channels of B, and 1.18, 1.25, and 1.25 bohr for those of N, resulting in plane wave cutoff 85 Ry. Partial core correction is included.

[52] T. Archer *et al.*, Phys. Rev. B **84**, 115114 (2011).

[53] H. J. Monkhorst and J. D. Pack, Phys. Rev. B **13**, 5188 (1976).

[54] M. T. Hutchings and E. J. Samuelsen, Phys. Rev. B **6**, 3447 (1972).

[55] R. Shanker and R. A. Singh, Phys. Rev. B **7**, 5000 (1973).